Eur. Phys. J. Plus (2021) 136:10
https://doi.org/10.1140/epjp/s13360-020-00980-x

THE EUROPEAN PHYSICAL JOURNAL PLUS

Regular Article

# Extended detrended fluctuation analysis: effects of nonstationarity and application to sleep data

**A. N. Pavlov**[1,2,a], **O. N. Pavlova**[1], **O. V. Semyachkina-Glushkovskaya**[1], **J. Kurths**[1,3,4]

[1] Saratov State University, Astrakhanskaya 83, Saratov, Russia 410012
[2] Regional Scientific and Educational Mathematical Center "Mathematics of Future Technologies", 23 Gagarina Avenue, Nizhny Novgorod, Russia 603950
[3] Potsdam Institute for Climate Impact Research, Telegraphenberg A 31, 14473 Potsdam, Germany
[4] Institute of Physics, Humboldt University Berlin, 12489 Berlin, Germany

Received: 11 October 2020 / Accepted: 30 November 2020


**Abstract** Extended detrended fluctuation analysis (EDFA) is a recently proposed modification of the conventional method, which provides a characterization of complex time series with varying nonstationarity. It evaluates two scaling exponents for a better quantification of inhomogeneous datasets. Here, we study the effect of different types of nonstationarity on these exponents, including trend, switching between processes with distinct statistical properties and energy variability. Using the simulated signals, we show that the first two types of nonstationarity have the strongest effect for anticorrelated processes and complicate their diagnosis. Nonstationarity in energy is more crucial for time series with positive long-range correlations. Next, we apply EDFA to rat experiments to study the activation of brain lymphatic drainage during sleep. Our analysis reveals significant distinctions in EDFA's measures between the background electrical activity of the brain and the stage of sleep. The latter offers an indirect way to identify and characterize the nightly activation of the drainage and clearance of brain tissue.

## 1 Introduction

Many processes in the dynamics of natural systems exhibit power-law statistics with long-range correlations. Their characterization is often used to understand the behavior of the system and reveal changes caused by variable external conditions or transitions between different types of complex dynamics. Correlation analysis of experimental data is restricted by two main problems: (i) decay of the correlation function that approaches zero, where computing errors strongly affect the quantification of power-law behavior, and (ii) nonstationarity of the measured time series associated with the sensitivity of the estimated quantities from the starting time moment. These circumstances led to detrended fluctuation analysis (DFA) [1,2], proposed to improve the correlation analysis of nonstationary time series. Its peculiarity consists in the transition from a decaying correlation function to a growing function (random walk or signal profile), whose power-law behavior is easier to characterize. The potentials and limitations of this approach were explored in subsequent works [3–6] using simulated

[a] e-mail: pavlov.alexeyn@gmail.com (corresponding author)

datasets. During the last decades, DFA has been treated as a quite universal approach in various experimental studies [7–14].

In its standard version described by Peng et al. [1,2], DFA includes partitioning of the signal profile into nonoverlapping segments with a detrending procedure that includes fitting the trend within each part and its extraction. The detrended profile can further be characterized in terms of root-mean-square (RMS) fluctuations, which usually increase with growing segment length. A piece-wise linear fitting is mainly used for this purpose, although other types of fitting are also applicable. Such approach is perfectly adapted for fairly homogeneous time series with similar trend features throughout the signal. However, often the real dynamics of complex systems is quite inhomogeneous, especially for transients: detrending is well-provided with small RMS fluctuations for some data segments, while these fluctuations are much larger for other segments. If the degree of nonstationarity varies significantly between different parts of the data, then few segments with the strongest nonstationarity can mainly affect the estimated quantities, and the role of other parts of the data becomes insufficient.

Slow changes in the local mean value treated as a trend are only one basic type of nonstationarity. The time-varying dynamics of natural systems involves a wider range of complex phenomena, including intermittent behavior, such as switching between states with distinct statistical properties, nonstationarity in energy, etc. These circumstances are the reason for the improvement of signal processing methods in order to expand their capabilities in describing the dynamics of inhomogeneous time series. Recently, we have proposed a modified approach for inhomogeneous time series that extends the conventional DFA by introducing an additional quantity characterizing the features of nonstationary behavior [15]. This extended DFA (EDFA) evaluates two scaling exponents, which provide better quantification of nonstationary datasets. In the original paper [15], we showed how this tool can be applied in physiology to diagnose responses to sudden jumps in blood pressure as an example. Here, we conduct a more thorough analysis of this tool for different types of nonstationarity presented in simulated time series by using several examples of random processes with known statistical properties. Then, we apply this tool to EEG data in rats to compare the features of slow-wave dynamics upon activation of the lymphatic drainage function. This problem requires consideration in the frequency range ($f < 1$ Hz), which is generally not taken into account when analyzing EEG rhythms. Such slow EEG components can affect the EDFA results, since they cause a higher nonstationarity of the signal profile, and therefore, knowledge of these effects is important for reliable analysis and interpretation of the estimated quantities. Sleep and lymphatics are crucial to preserve the health of the central nervous system [16–21]. Sleep is important for clearance of metabolites and neurotoxins [16]. It produces changes in oscillations of brain fluids accompanied by specific slow wave patterns in EEG [17]. Based on a series of experiments, we report significant distinctions between awake and sleep states in terms of long-range memory effects. These results can serve as indirect evidence of night activation of brain tissue drainage and clearance effects. The ability to stimulate lymph flow in the sleeping brain is likely to play an important role for the developing of innovative methods of neurorehabilitation therapy.

The paper is organized as follows. Section 2 briefly discusses the detrended fluctuation analysis and its extension, EDFA, the potentials and limitations of which are studied on the basis of simulated and experimental data. Section 3 describes three types of nonstationarity, which are considered using several examples of noises with known statistical properties. We discuss their effect on the quantification of long-range correlations and apply EDFA to analyze the slow-wave dynamics in nonstationary EEG records in the state of wakefulness and sleep in rats. Section 4 summarizes the main results and conclusions.

## 2 Extended detrended fluctuation analysis (EDFA)

The conventional DFA [1,2] includes the following main steps:

(1) Construction of a random walk or profile of a given signal $x(i)$, $i = 1, \ldots, N$

$$y(k) = \sum_{i=1}^{k} [x(i) - \langle x \rangle], \quad \langle x \rangle = \sum_{i=1}^{N} x(i). \tag{1}$$

(2) Separation of $y(k)$ into segments of length $n$, and a piece-wise linear fitting the local trend $y_n(k)$ within each segment.

(3) Evaluation of the RMS fluctuations for the selected $n$

$$F(n) = \sqrt{\frac{1}{N} \sum_{k=1}^{N} [y(k) - y_n(k)]^2}. \tag{2}$$

(4) Steps 2 and 3 are repeated in a wide range of $n$ to establish the power-law behavior

$$F(n) \sim n^{\alpha} \tag{3}$$

and determine the scaling exponent $\alpha$. Usually, $n \ll N$ (in our estimations, $n \leq 0.1N$). As described in the Introduction, this approach is well-adapted for datasets, where the trend features are quite similar among different segments. Otherwise, $F(n)$ becomes sensitive to the presence of segments with the strongest nonstationarity compared to other parts of the data. To describe the inhomogeneity of trend features throughout the signal, we introduced the measure

$$dF(n) = \max [F_{loc}(n)] - \min [F_{loc}(n)], \tag{4}$$

where $F_{loc}(n)$ are local RMS fluctuations of the profile $y(k)$ around the trend $y_n(k)$, which are estimated within each segment. The difference $dF(n)$ quantifies the distinctions between these local RMS fluctuations. If the trend or other types of nonstationarity have similar properties, then $dF(n)$ takes small values. Otherwise, some segments give $F_{loc}(n)$ near zero, and $dF(n)$ approach to $\max [F_{loc}(n)]$. According to our recent study [15], $dF(n)$ often exhibits power-law behavior, whose scaling exponent differs from $\alpha$,

$$dF(n) \sim n^{\beta}. \tag{5}$$

This approach is called extended DFA (EDFA) [15]. Although its applications confirm that a better characterization of nonstationary datasets is provided by computing both exponents, $\alpha$ and $\beta$, the role of different types of nonstationarity on these quantities has not been studied previously. In Sect. 3, we provide such an analysis and apply EDFA to quantify the slow-wave dynamics in EEG data.

## 3 Results and discussion

Using simulated datasets, we discuss here three types of nonstationarity: variations of the local mean value (type 1), switching between different processes (type 2), and nonstationarity in energy (type 3). We choose also three examples of stochastic processes, namely

- white noise (uncorrelated process with $\alpha = 0.5$),
- $1/f$ noise (correlated process with $\alpha = 1.0$),

- noise with anti-correlations (we examined the derivative of $1/f$-noise, $\alpha \approx 0.1$).

In numerical simulations, intensities of these processes are adjusted in such a way that the ranges of random values approximately correspond to each other.

### 3.1 The first type of nonstationarity: low-frequency variations

As the first type of nonstationarity consider slow changes in the local mean value (low-frequency variations treated as trend), for this purpose, a harmonic function $A\sin(\omega t)$ with a very low frequency $\omega$ and amplitude $A$ was added to each stochastic process. The frequency was selected in such a way that the whole recording (64,000 samples) included 2–3 periods of oscillations, and the data segments analyzed within the EDFA contained small parts of one period only. The latter allows us to interpret these parts as a trend.

Let us consider the results for a fixed value of the amplitude ($A = 0.03$) using white noise with the standard deviation $\sigma = 0.075$ as an example. Figure 1a, b demonstrates the dependencies $F(n)$ and $dF(n)$ in the double logarithmic plot. Without an additive signal leading to variations in the local mean value, the scaling exponents $\alpha$ coincide in the ranges $\lg n < 3.0$ and $\lg n > 3.0$ ($\alpha \sim 0.5$, Fig. 1a). When harmonic oscillations are added to white noise, the $\alpha$ exponent does not change in the first range, but it increases significantly for larger $\lg n$. A similar behavior is observed for the $\beta$ exponent (Fig. 1b). The latter usually takes values less than $\alpha$, but the behavior is similar; the trend does not significantly affect the estimations for $\lg n < 3.0$, but the local slope $\lg dF$ *vs* $\lg n$ changes for $\lg n > 3.0$. Due to this, we evaluate two local values of each scaling exponent, in the range $\lg n < 3.0$ (respectively, $\alpha_1$ and $\beta_1$) and in the range $\lg n > 3.0$ ($\alpha_2$ and $\beta_2$).

Figure 1c, d shows how these exponents depend on the amplitude of the harmonic function. This slow trend does not affect the values of $\alpha_1$ and $\beta_1$, which are computed using short data segments (less than 1/25-th part of the period $T = 2\pi/\omega$ corresponding to $\lg n < 3.0$). According to Figure 1c, d, these quantities do not change with increasing amplitude $A$. However, a slow nonstationarity has a more pronounced effect on both scaling exponents in the range $\lg n > 3.0$. Note that $\alpha_2$ increases about 3.3 times at the maximum value of $A$ in Fig. 1c, while $\beta_2$ increases even stronger (5 times). The latter can produce misinterpretations. Without preliminary filtering, stochastic process with $\alpha_1 = 0.5$ and trend can be treated as a process which is close to Brownian noise ($\alpha_2 = 1.5$) or even to a "smoother" random process. The standard deviation of white noise in this example is $\sigma = 0.075$, and the random values are mainly associated with the range $[-0.2, 0.2]$ (inset in Fig. 1c), therefore, $A \leq \sigma$.

To establish how strong are the variations of the scaling exponents for stochastic processes under study, we consider their changes with increasing amplitude $A$ of the harmonic function instead of the absolute values of $\alpha$ and $\beta$. Figure 2 shows the differences $\alpha - \alpha_0$ and $\beta - \beta_0$, where $\alpha$ and $\beta$ are the exponents estimated in the range $\lg n > 3.0$ (for convenience, we omit the index 2, since only this range is further analyzed, where nonstationarity affects the results), and $\alpha_0$ and $\beta_0$ are the values of scaling exponents, which correspond to stationary processes (i.e., related to $A = 0$). In accordance with Fig. 2, both exponents show similar behavior with growing $A$. The strongest changes occur for the anticorrelated random process ($\alpha_0 = 0.1$). With larger $\alpha_0$, changes become less pronounced. For white noise, e.g., the differences $\alpha - \alpha_0$ and $\beta - \beta_0$ decrease compared to the anticorrelated process, and among the considered examples, $\alpha - \alpha_0$ and $\beta - \beta_0$ take the minimum values for $1/f$ noise. Note that a similar conclusion follows from the analysis of other random processes (not shown in this paper). Thus, we can state that the presence of a trend has a stronger effect on the quantification of anticorrelated processes, and it is weaker for "smoother" processes characterized by larger scaling exponent $\alpha_0$. A comparison of Fig. 2a, b also makes it possible to conclude that the

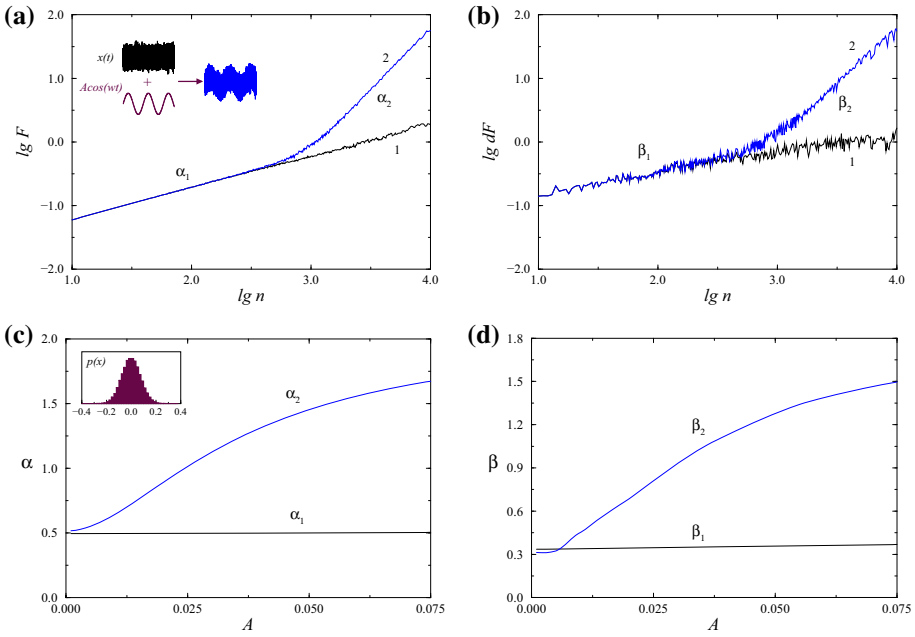


**Fig. 1** Analysis of white noise with the added harmonic function $A\sin(\omega t)$. Estimates of the scaling exponents $\alpha$ (**a**) and $\beta$ (**b**) are given without (dependencies 1, $A = 0$) and with (dependencies 2, $A = 0.03$) this slow variation of the local mean value. The slopes differ significantly for long-range ($\lg n > 3.0$) and shorter ($\lg n < 3.0$) correlations (**a**), and a similar effect occurs for the exponent $\beta$ (**b**). The corresponding local values of each scaling exponent depending on the amplitude $A$ of the harmonic function are shown in (**c**, **d**)

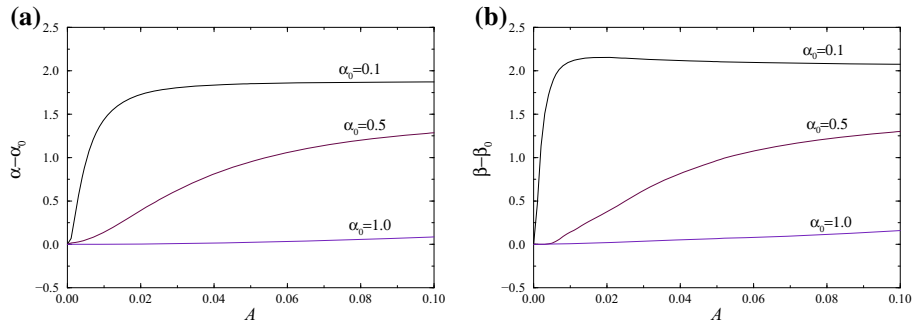


**Fig. 2** Changes in the scaling exponents $\alpha$ (**a**) and $\beta$ (**b**) in the range $\lg n > 3.0$ for three stochastic processes provoked by a slow harmonic variation of the local mean value. The differences $\alpha - \alpha_0$ and $\beta - \beta_0$ are computed from the values $\alpha_0$ and $\beta_0$ related to $A = 0$

exponent $\beta$ changes more strongly for small amplitudes $A$ as compared to $\alpha$, i.e., $\beta$ is more sensitive to the presence of nonstationarity.

### 3.2 The second type of nonstationarity: switching

As the second type of nonstationarity, switching between two random processes with different statistical characteristics is selected, which is illustrated by the inset in Fig. 3a. Here, a

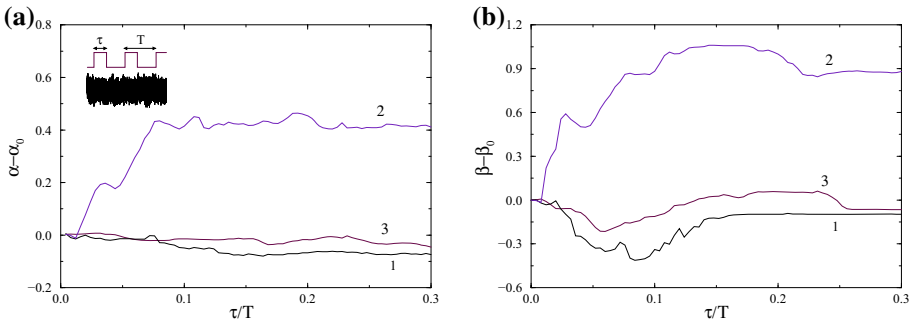


**Fig. 3** Changes in the scaling exponents $\alpha$ (**a**) and $\beta$ (**b**) in the range $\lg n > 3.0$ for three stochastic processes caused by switching between white noise and anti-correlated random process (1), white noise and $1/f$-noise (2), $1/f$-noise and noise with anti-correlations (3). The differences $\alpha - \alpha_0$ and $\beta - \beta_0$ are given depending on the $\tau/T$ ratio

visual inspection of $x(t)$ may not reveal changes in the signal, because the range of $x$ does not vary during switching. However, $x(t)$ contains alternation of data segments when one random process includes segments of the second process of duration $\tau$. We consider periodic switching (with period $T$) and analyze the results depending on the $\tau/T$ ratio.

Three cases, namely the switching between white noise and anti-correlated random process, white noise and $1/f$-noise, $1/f$-noise and noise with anti-correlations are shown in Fig. 3. Alternations between segments of white noise and noise with anti-correlations (dependencies 1 in Fig. 3) produce a relatively small shift in the $\alpha$ exponent from the level $\alpha_0 = 0.5$, which is related to uncorrelated process. Changes in $\beta$ are stronger, and this exponent decreases from about 0.3 to negative values. The most pronounced reactions occur when $\tau$ is chosen near $T/10$. Alternations between white noise and $1/f$ noise (dependences 2) lead to a shift of $\alpha$ from $\alpha_0 = 0.5$ for short segments of $1/f$ noise to about 1 when segments of each random process are comparable. In this example, the exponent $\beta$ varies from negative values to about 0.7. Switching between $1/f$ noise and noise with anti-correlations (dependences 3) does not produce strong changes of both exponents depending on $\tau$. To clearly show and compare the effects, we again demonstrate in Fig. 3 the differences in the exponents $\alpha - \alpha_0$ and $\beta - \beta_0$. According to this figure, we can conclude that a process with a larger $\alpha_0$ has a stronger effect on the estimated characteristics of long-range correlations. Thus, if we choose the process with anti-correlations as the basic one, then the presence of segments with correlated behavior leads to much stronger changes in the scaling exponents $\alpha$ and $\beta$. This is in accordance with the conclusions of recent studies [11,12] on the higher sensitivity of anticorrelated processes to the presence of artifacts and missing data. As in the previous case (Sect. 3.1), $\beta$ is more sensitive to the presence of nonstationarity compared to $\alpha$.

### 3.3 The third type of nonstationarity: jumps in energy

The third type of nonstationarity also includes changes in the signal structure for some segments, but now they are caused by jumps in energy (e.g., noise intensity) instead of switching between processes with different correlation properties. The corresponding examples are shown in Fig. 4, where two intensities are considered for each noise and the results are analyzed depending on their ratio.

For white noise, the changes in the $\alpha$ exponent in the range $\lg n > 3.0$ are about 15% for the maximal ratio $I_2/I_1 = 9$ compared to a stationary process ($I_2/I_1 = 1$), while the $\beta$

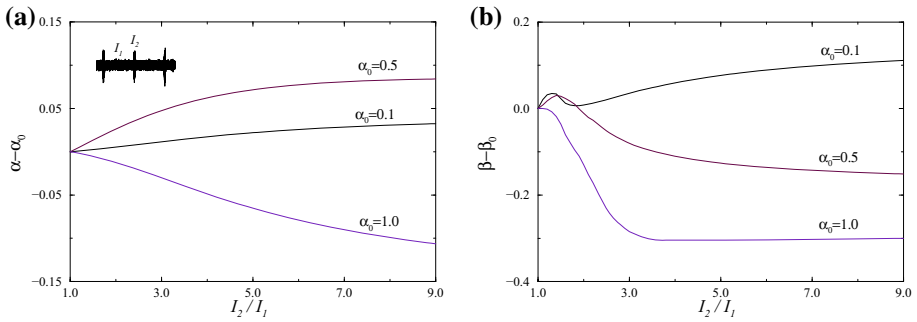


**Fig. 4** Changes in the scaling exponents $\alpha$ (**a**) and $\beta$ (**b**) in the range $\lg n > 3.0$ for three stochastic processes caused by jumps in energy depending on the ratio of noise intensities

exponent reduces by about 40%. A change in $\alpha$ by 0.1 is observed for $1/f$ noise; however, $\alpha$ decreases in the latter case with the ratio $I_2/I_1$. The related changes in $\beta$ are 3 times stronger. For noise with anti-correlations, $\beta$ takes only negative values, while in other examples of stochastic processes $\beta > 0$. The $\alpha$ exponent varies within 0.03. Thus, unlike previous types of time-varying behavior, nonstationarity in energy has a weaker effect on the results of the conventional DFA method as applied to anticorrelated processes. The evaluation of $\beta$ again more clearly shows changes in the signal structure.

### 3.4 Analysis of experimental data

In the dynamics of natural systems, e.g., in life sciences, several types of nonstationarity can coexist, and their extraction or correction is a difficult problem even for the simplest type of nonstationarity, a trend. Complex dynamics of such systems does not always enable removing low-frequency variations of the local mean value, e.g., when studying slow wave oscillations of physiological control systems. In the latter case, it is often unclear how to distinguish between rhythms of interest and a trend. Generally, a trend is associated with the frequency band below the rhythms under study. Its removing with a high-pass filter does not affect faster dynamics, but the influence of this trend on the quantification of system state is avoided. Such a filtering may be inappropriate when studying slow dynamics. Here, we consider one such example, namely the activation of the brain lymphatic drainage function during sleep. This activation is associated with indications in the frequency range $f < 1$ Hz which is generally not included in usual analyses of EEG-rhythms. Without a preliminary filtering of data, we cannot be sure that nonstationary parts of data will not influence the results of EDFA.

Our analysis is based on experiments performed in nine adults male Wistar rats using two-channels EEG-recordings in awake animals (normal conditions) and during sleep. The experiments were carried out in accordance with the Guide for the Care and Use of Laboratory Animals (8th edition. Washington: The National Academies Press, 2011). The protocols were approved by the local ethics committee at the Saratov State University. All measurements were performed with a sampling rate 2 kHz. The removal of artifacts was carried out using the method [22]. Then, we selected 10-minute segments with a more homogeneous structure. Identical conditions of physiological measurements are considered for all recordings (more experimental details are given in [23]). Therefore, even if a nonstationarity affects the absolute values of the scaling exponents, their variations between the states reflect changes caused by

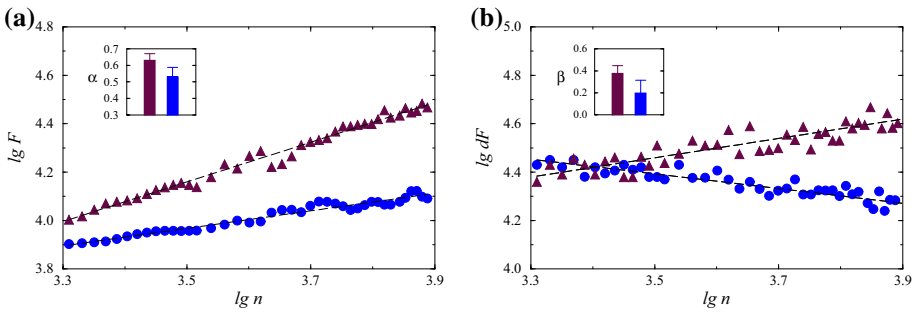


**Fig. 5** An example of a decrease in the scaling exponents $\alpha$ (**a**) and $\beta$ (**b**) for the sleep stage (circles) compared to the background electrical activity of the brain in an awake rat. The insets show the results of statistical analysis ($mean \pm SE$), which confirm this decrease for a group of rats

the dynamics. Application of EDFA reveals distinctions in both scaling exponents. Unlike the $\alpha$ exponent of the conventional DFA which is usually reduced during the sleep, the $\beta$ exponent can change its sign and become negative in the range of large $\lg n$ (Fig. 5). Here, $\alpha$ decreases from 0.78 to 0.43, quantifying a change of the correlation type (positive power-law correlations in an awake animal, and anti-correlations during sleep). The $\beta$-exponent decreases from 0.41 till $-0.29$.

An analogous effect is obtained for the whole group of animals. Insets in Fig. 5 show results of our statistical analysis of recordings related to awake and sleep states which confirm significant distinctions for both exponents (the Mann–Whitney test, $p < 0.05$). Thus, normal sleep affects the long-term memory in the EEG data. Based on the previous studies performed with different in vivo techniques (magnetic resonance imaging, two-photon microscopy, fluorescence analysis) and ex vivo methods (confocal and spectrofluorimetric analyses), it was shown that an activation of cleaning function of the cerebral lymphatics is related with opening of the blood-brain barrier [19,21]. This activation can be caused by different reasons, and normal sleep is one of them. Analysis of the corresponding processes can be provided with EDFA of EEG data which represents an indirect way to detect reactions in the long-term memory associated with activation of the cerebral lymphatics that is necessary to keep the homeostasis of the central nervous system via cleaning of the brain tissues.

## 4 Conclusion

We analyzed how several types of nonstationarity affect the characterization of time series with the recently proposed EDFA method. For this purpose, the role of trend, switching between two different processes and variability in energy using three stochastic processes with different correlation properties was discussed. Each of these types of nonstationarity provides a change of the scaling exponents related to the long-range correlations. Slow variations in the local mean value associated with the trend have a strong effect on anti-correlated processes and produce a significant shift in both exponents, $\alpha$ and $\beta$. With an increase in $\alpha$ and the related transition from anti-correlations to positive power-law correlations, changes in exponents become less pronounced. In the case of switching between stochastic processes, the scaling exponents take values which are closer to the exponents of a process with larger $\alpha_0$, i.e., the $\alpha$ exponent in the absence of switching. These results are consistent with recent studies of higher sensitivity of anticorrelated processes to artifacts, noise and data loss. Therefore, the first two

types of nonstationarity complicate the diagnosis of anti-correlated processes. Unsteadiness in energy has a different effect. Although it changes the characteristics of all signals, a stronger shift in the scaling exponent takes place for time series with positive long-range correlations. The results obtained show that knowledge of the effects of nonstationarity is crucial for the reliable characterization of complex processes. Despite the opinion that DFA can be applied to experimental data without preliminary processing, the elimination of nonstationarity at the first stage (if this procedure is possible) is an important task that can essentially improve the reliable interpretation of the results. Note that the $\beta$ exponent is significantly more sensitive to all types of nonstationarity.

In addition to the simulation results, we also examined the application of EDFA to EEG recordings in rats to characterize the activation of brain lymphatic drainage during sleep. Such a problem is an example of tasks where slow dynamics should be considered, and preliminary data filtering should be avoided to analyze dynamics in the frequency range $f < 1$ Hz. This means that slow nonstationarity may affect the results, but the measurement conditions are the same for all animals. Despite estimates of the scaling exponents can be affected by trend, differences between awake and sleep states are a consequence of distinctions in the slow-wave dynamics. Our analysis revealed significant distinctions for both scaling exponents, and this approach can be treated as an indirect way to characterize the nightly activation of cerebral lymphatics and cleansing effects.

**Acknowledgements** Theoretical studies with simulated datasets were supported by the Russian Science Foundation (Agreement 19-12-00037). Analysis of experimental data in Sect. 3.4 was supported by the RF Government Grant No. 075-15-2019-1885.

## References

1. C.-K. Peng, S.V. Buldyrev, S. Havlin, M. Simons, H.E. Stanley, A.L. Goldberger, Phys. Rev. E **49**, 1685 (1994)
2. C.-K. Peng, S. Havlin, H.E. Stanley, A.L. Goldberger, Chaos **5**, 82 (1995)
3. K. Hu, PCh. Ivanov, Z. Chen, P. Carpena, H.E. Stanley, Phys. Rev. E **64**, 011114 (2001)
4. Z. Chen, PCh. Ivanov, K. Hu, H.E. Stanley, Phys. Rev. E **65**, 041107 (2002)
5. R.M. Bryce, K.B. Sprague, Sci. Rep. **2**, 315 (2012)
6. Y.H. Shao, G.F. Gu, Z.Q. Jiang, W.X. Zhou, D. Sornette, Sci. Rep. **2**, 835 (2012)
7. K. Ivanova, M. Ausloos, Physica A **274**, 349 (1999)
8. C. Heneghan, G. McDarby, Phys. Rev. E **62**, 6103 (2000)
9. P. Talkner, R.O. Weber, Phys. Rev. E **62**, 150 (2000)
10. J.W. Kantelhardt, E. Koscielny-Bunde, H.H.A. Rego, S. Havlin, A. Bunde, Physica A **295**, 441 (2001)
11. Q.D.Y. Ma, R.P. Bartsch, P. Bernaola-Galván, M. Yoneyama, PCh. Ivanov, Phys. Rev. E **81**, 031101 (2010)
12. O.N. Pavlova, A.S. Abdurashitov, M.V. Ulanova, N.A. Shushunova, A.N. Pavlov, Commun. Nonlinear Sci. Numer. Simul. **66**, 31 (2019)
13. N.S. Frolov, V.V. Grubov, V.A. Maksimenko, A. Lüttjohann, V.V. Makarov, A.N. Pavlov, E. Sitnikova, A.N. Pisarchik, J. Kurths, A.E. Hramov, Sci. Rep. **9**, 7243 (2019)
14. O.N. Pavlova, A.N. Pavlov, Physica A **536**, 22586 (2019)
15. A.N. Pavlov, A.S. Abdurashitov, A.A. Koronovskii Jr., O.N. Pavlova, O.V. Semyachkina-Glushkovskaya, J. Kurths, Commun. Nonlinear Sci. Numer. Simul. **85**, 105232 (2020)
16. L. Xie, H. Kang, Q. Xu, M.J. Chen, Y. Liao, M. Thiyagarajan, J. O'Donnell, D.J. Christensen, C. Nicholson, J.J. Iliff, T. Takano, R. Deane, M. Nedergaard, Science **342**, 373 (2013)
17. S. Da Mesquita, Z. Fu, J. Kipnis, Neuron **100**, 375 (2018)
18. N.E. Fultz, G. Bonmassar, K. Setsompop, R.A. Stickgold, B.R. Rosen, J.R. Polimeni, L.D. Lewis, Science **366**, 628 (2019)
19. O. Semyachkina-Glushkovskaya, A. Abdurashitov, A. Dubrovsky, D. Bragin, O. Bragina, N. Shushunova, G. Maslyakova, N. Navolokin, A. Bucharskaya, V. Tuchin, J. Kurths, A. Shirokov, J. Biomed. Opt. **22**, 121719 (2017)

20. O. Semyachkina-Glushkovskaya, D. Postnov, J. Kurths, Int. J. Mol. Sci. **19**, 3818 (2018)
21. O. Semyachkina-Glushkovskaya, V. Chehonin, E. Borisova, I. Fedosov, A. Namykin, A. Abdurashitov, A. Shirokov, B. Khlebtsov, Y. Lyubun, N. Navolokin, M. Ulanova, N. Shushunova, A. Khorovodov, I. Agranovich, A. Bodrova, M. Sagatova, A.E. Shareef, E. Saranceva, T. Iskra, M. Dvoryatkina, E. Zhinchenko, O. Sindeeva, V. Tuchin, J. Kurths, J. Biophoton. **11**, e201700287 (2018)
22. N.P. Castellanos, V.A. Makarov, J. Neurosci. Methods **158**, 300 (2006)
23. A.N. Pavlov, A.I. Dubrovsky, A.A. Koronovskii Jr., O.N. Pavlova, O.V. Semyachkina-Glushkovskaya, J. Kurths, Chaos **30**, 073138 (2020)